

Decoupling Skeleton and Flesh: Efficient Multimodal Table Reasoning with Disentangled Alignment and Structure-aware Guidance

Yingjie Zhu^{1,2} Xuefeng Bai¹ Kehai Chen¹ Yang Xiang² Youcheng Pan² Xiaoqiang Zhou² Min Zhang¹

Abstract

Reasoning over table images remains challenging for Large Vision-Language Models (LVLMs) due to complex layouts and tightly coupled structure–content information. Existing solutions often depend on expensive supervised training, reinforcement learning, or external tools, limiting efficiency and scalability. This work addresses a key question: *how to adapt LVLMs to table reasoning with minimal annotation and no external tools?* Specifically, we first introduce DiSCO, a Disentangled Structure–Content alignment framework that explicitly separates structural abstraction from semantic grounding during multimodal alignment, efficiently adapting LVLMs to tables structures. Building on DiSCO, we further present Table-GLS, a Global-to-Local Structure-guided reasoning framework that performs table reasoning via structured exploration and evidence-grounded inference. Extensive experiments across diverse benchmarks demonstrate that our framework efficiently enhances LVLM’s table understanding and reasoning capabilities, particularly generalizing to unseen table structures.

1. Introduction

Tables are structured data representations that systematically organize information into rows and columns, serving as a fundamental medium for conveying relational data across numerous domains such as financial reports, scientific articles, medical records and government documents (Chen et al., 2021; Akhtar et al., 2022; Cheng et al., 2022; Li et al., 2024). Recent advances in large foundation models have provided new modeling paradigms for automated table understanding. In particular, Large Vision-Language Models (LVLMs) (Liu et al., 2024a; Bai et al., 2025a) integrate visual perception with language modeling, enabling unified

¹Harbin Institute of Technology, Shenzhen, China ²Peng Cheng Laboratory, Shenzhen, China. Correspondence to: Xuefeng Bai <baixuefeng@hit.edu.cn>.

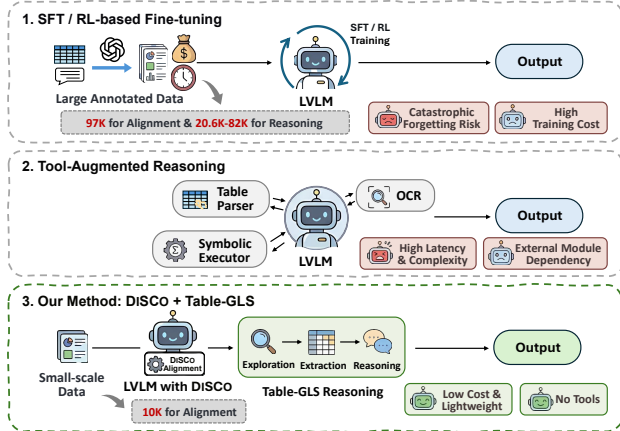


Figure 1. Comparison of our framework with current methods.

processing of table images and scanned documents for real-world applications, and providing a unified framework for interpreting table images and answering natural language questions about their content (Zheng et al., 2024; Fu et al., 2025). Despite their success on various vision-language tasks (Alayrac et al., 2022; Bai et al., 2025b; Zhu et al., 2025), LVLMs still struggle with table understanding and reasoning—particularly when tables exhibit complex layouts, dense data, or intricate structural dependencies.

Current methods for adapting LVLMs to table reasoning largely follow two paradigms. The first relies on extensive supervised fine-tuning (Zheng et al., 2024; Zhao et al., 2024; Zhou et al., 2025) or reinforcement learning-based optimization (Kang et al., 2025; Jiang et al., 2025) to equip models with table reasoning capabilities. While often effective, this paradigm is constrained by the need for costly and scarce expert annotations for table reasoning data, which limits scalability and risks catastrophic forgetting of the model’s original reasoning skills. The second category augments LVLMs with external tools—such as visual editors or symbolic modules—to explicitly steer visual attention and reasoning steps (Fu et al., 2025). Nevertheless, these methods increase system complexity and inference latency, failing to enhance the model’s intrinsic capacity for structural understanding and reasoning. These limitations motivate a key research question:

Is there a way to adapt LVLMs to table reasoning with minimal annotation cost and without external tools?

In this paper, we address this question by introducing an efficient framework that adapts LVLMs to table reasoning without expensive reasoning-specific annotations or auxiliary tools, as shown in Figure 1. The key idea is to transfer the intrinsic textual-semantic reasoning capability of LVLMs to table structure through two explicit design principles: decoupling structural perception from semantic grounding, and performing structure-aware reasoning via a global-to-local chain. Specifically, we first propose a **Disentangled Structure–Content (DiSCO)** alignment framework that explicitly separates structure learning from content grounding during multimodal alignment. Concretely, our approach decomposes multimodal table understanding into complementary alignment objectives, i.e., structure alignment that learns table layouts independent of cell content, and semantic alignment that grounds table content through global and local natural language descriptions. This disentanglement not only facilitates the transfer of the LVLM’s existing knowledge to the table content but also enables more data-efficient and targeted adaptation to table structures. Building upon the enhanced representations learned by DiSCO, we further introduce **Table-GLS**, a **Global-to-Local Structure-guided reasoning** method that performs multimodal table reasoning in a step-by-step yet lightweight manner without additional fine-tuning or external tools. Instead of directly predicting answers, Table-GLS guides the LVLM to first explore the global table structure and identify task-relevant row and column indices, then extract a minimal sub-table as verifiable evidence. The final reasoning is performed based on the extracted sub-table, reducing spurious correlations and improving robustness.

Extensive experiments on 21 table understanding and reasoning tasks demonstrate that the proposed methods achieve improvements on both table understanding and reasoning, using only 10K table images for alignment. DiSCO effectively enhances structure- and content-aware understanding, while Table-GLS effectively guides LVLMs for reliable table reasoning. The combined framework delivers further performance gains on challenging multimodal table tasks, particularly for tables with unseen table structures. Our contributions can be summarized as follows:

- We propose DiSCO, a disentangled structure–content alignment framework that improves LVLMs’ understanding of table structure and content, especially for complex and unseen table layouts.
- We introduce Table-GLS, a global-to-local structure-aware inference framework that enables accurate table reasoning at inference time without external tools or

additional reasoning-oriented fine-tuning.

- The proposed methods achieve robust improvements in understanding and reasoning across 21 tasks and benchmarks, particularly on unseen table structures¹.

2. Related Work

2.1. Table Modeling

Table modeling based on language models has been widely studied, with a predominant focus on table serialization, which converts 2D tables into linear text sequences. Representative methods include row-wise serialization (e.g., TaPas (Herzig et al., 2020), TUTA (Wang et al., 2021)), structure-aware formats with special tokens (e.g., TaPEX (Liu et al., 2022)), and hybrid row–column schemes (e.g., TABBIE (Iida et al., 2021)). With the rise of LLMs, recent studies explore applying general-purpose language models (e.g., LLaMA, Gemma) to tabular tasks by first converting tables into textual formats such as CSV, JSON, Markdown, or HTML (Borisov et al., 2022). While effective, these approaches encode table structure and semantic content in an entangled manner and often suffer from scalability issues under long-context modeling (Sui et al., 2024). For LVLMs, existing methods typically rely on supervised fine-tuning or reinforcement learning (e.g., GRPO) to align table images with textual representations such as HTML, Markdown, or LaTeX, implicitly coupling structure and content during training (Zheng et al., 2024; Zhou et al., 2025; Kang et al., 2025; Jiang et al., 2025). In contrast, our work introduces a disentangled structure–content representation that enables more controllable and generalizable table understanding and reasoning in multimodal settings.

2.2. Multimodal Table Understanding and Reasoning

Recent research on multimodal table understanding and reasoning primarily focus on dataset construction, unified multimodal modeling, and enhanced reasoning supervision across diverse table-centric tasks. Representative benchmarks and pretraining corpora, such as MMTab (Zheng et al., 2024), TabPedia (Zhao et al., 2024), and SynTab (Zhou et al., 2025), support diverse table perception and reasoning tasks, with models like Table-LLaVA (Zheng et al., 2024) strengthening joint visual–tabular representations via cell-level alignment. Beyond generic tables, works including Multimodal ArXiv (Li et al., 2024) and MMTBENCH (Titiya et al., 2025) extend multimodal table reasoning to scientific documents and complex real-world scenarios by modeling fine-grained interactions among tables, charts, text, and

¹Our data and code are available at <https://github.com/AAAndy-Zhu/TableVLM>

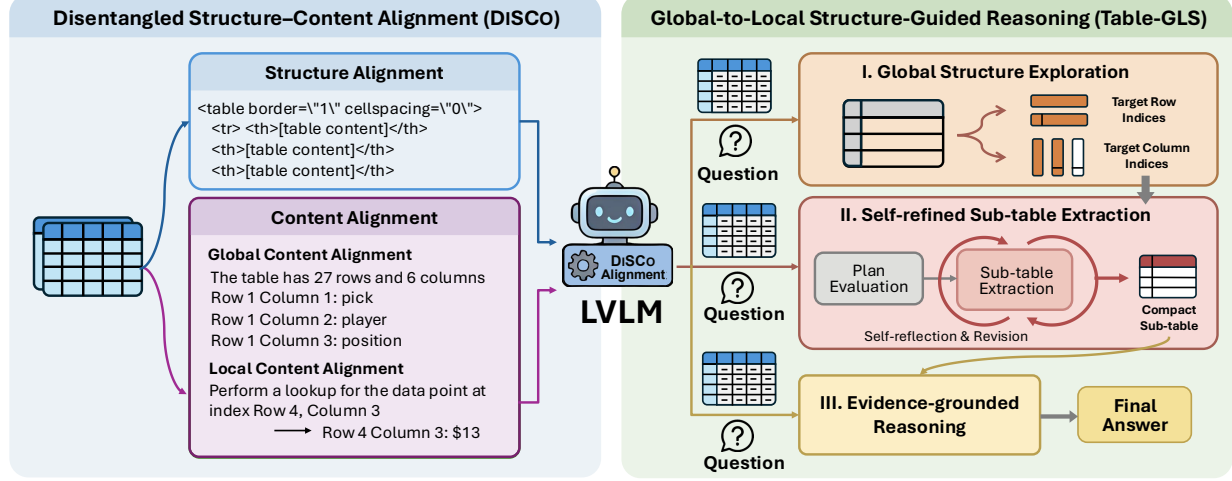


Figure 2. Overall framework of DiSCO and Table-GLS.

other visual elements. To improve reasoning ability, recent methods introduce self-training or reinforcement learning signals, as exemplified by R3V (Cheng et al., 2025), Table-R1 (Kang et al., 2025), and TURBO (Jiang et al., 2025), which leverage reasoning trajectories or structure-aware rewards to optimize multimodal table reasoning during training. In contrast, inference-time approaches, such as REFOCUS (Fu et al., 2025), enable explicit multi-hop visual reasoning via external visual editing and code-driven control. Unlike current methods, which either rely on heavy training supervision or introduce additional tools, our work enhances LVLMs’ table understanding and reasoning by strengthening their intrinsic structure–content modeling and enabling lightweight, structure-guided reasoning at inference time.

3. Methodology

We propose an efficient and unified framework for multimodal table understanding and reasoning that strengthens LVLMs at both the representation and inference levels. The **core idea** is that disentangling structure abstraction from semantic grounding during multimodal alignment allows LVLMs to transfer their inherent understanding and reasoning ability to table images in a data-efficient manner. Thus, as illustrated in Figure 2, we first introduce DiSCO (§3.1), which performs disentangled structure–content alignment to enhance table structure learning by explicitly decoupling structure abstraction from semantic grounding during multimodal alignment. Then, we propose Table-GLS (§3.2), a global-to-local, structure-guided reasoning framework that performs inference by progressively identifying relevant table regions and reasoning over compact sub-tables. Together, DiSCO and Table-GLS form an efficient approach for adapting LVLMs

to multimodal table reasoning.

3.1. Disentangled Structure–Content Alignment

Tables naturally combine **structural organization** (e.g., rows, columns, and cell layout) with **semantic content** (e.g., the textual values within cells) (Lu et al., 2025). However, existing LVLM-based table alignment methods typically align table images with *linearized textual representations*, such as HTML, Markdown, or LaTeX. While these formats preserve both structure and content, they inevitably entangle layout cues with cell semantics into a single sequence, forcing the model to learn structural relations and semantic meanings simultaneously during alignment. This tightly coupled supervision obscures the distinct roles of structure and content, leading to inefficient learning and poor transfer across table layouts. Thus, we propose DiSCO, which disentangles structure abstraction from semantic grounding during alignment, enabling LVLMs to leverage their existing semantic understanding ability and adapt to table structures with minimal additional supervision.

Structure Alignment. To explicitly model table structure, we perform structure alignment using supervision that focuses solely on layout and relational organization, independent of cell semantics. Specifically, We derive a structure representation T_S by anonymizing all cell contents in conventional textual table sequences T , i.e. HTML, Markdown and LaTeX, using a unified placeholder token t_p , preserving only layout-related tokens such as row and column delimiters, hierarchical headers, and span markers:

$$T_S = \text{Anonymize}(T, t_p) \quad (1)$$

Given an instruction I_S and a table image V , the goal of structure alignment is to train the LVLMs to predict T_S

conditioned on the visual input, without access to semantic cell values. The training objective is formulated as

$$\mathcal{L}_{\text{struct}} = -\mathbb{E}_{(I_S, V, T)} \log P_\theta(T_S | I_S, V). \quad (2)$$

This objective forces the LVLM to focus on extracting and organizing structure information directly from the table image, rather than memorizing or entangling semantic content. As a result, the learned representations capture table layout more explicitly, providing a robust structure foundation for subsequent content grounding and reasoning.

Content Alignment. While structure understanding provides the foundation for table reasoning, accurate interpretation of semantic content is equally critical. Therefore, we design new content alignment objectives that explicitly condition semantic prediction on global and local structure context. Specifically, at the global level, the LVLM is instructed to produce a lightweight **semi-structured description** T_G of the table, including the total number of rows and columns, followed by a concise summary of what each row and column contains.

$$\mathcal{L}_{\text{content_global}} = -\mathbb{E}_{(I_G, V, T_G)} \log P_\theta(T_G | I_G, V), \quad (3)$$

where I_G and V represent the input instruction and the table image, respectively. This task encourages the model to associate semantic meanings with structural axes, rather than individual cells in isolation.

At the local level, we further introduce targeted content querying. Given a specified row index m and column index n , the LVLM is trained to identify and describe the textual content associated with that structural unit, such as *Row m Column n: [content]*. Thus the training objective for local content alignment is defined as

$$\mathcal{L}_{\text{content_local}} = -\mathbb{E}_{(I_L, V, m, n, T_L)} \log P_\theta(T_L | I_L, V, m, n), \quad (4)$$

where T_L denotes the textual content corresponding to the queried row and column. By separating content alignment from structure abstraction, this design compels the LVLM to ground semantics onto explicit structural coordinates learned during structure alignment. Together, global and local content alignment enable LVLMs to form disentangled yet complementary representations of table structure and content, crucial for robust multimodal table understanding and reasoning. More details are description in Appendix B.

3.2. Global-to-Local Structure-Guided Reasoning

Building upon DISCO, we introduce a Global-to-Local Structure-Guided Reasoning (Table-GLS) framework to guide LVLMs progressively reason on table structures. Different from exist methods which require extensive training or external tools, Table-GLS operates in a

training-free and tool-free manner. As shown in Figure, Table-GLS guides the reasoning process through a three-stage mechanism, i.e., (I) Global Structure Exploration, (II) Self-refined Sub-table Extraction and (III) Evidence-grounded Reasoning.

Global Structure Exploration. Table-GLS starts with global structure exploration. Given a table image V and a question q , the LVLM is prompted with instruction I_{GSE} to analyze the overall table layout, including headers, row labels, and their semantic roles, and to determine the structural regions that are most relevant to the task,

$$T_t, R, C = \text{LVLM}(I_{GSE}, V, q), \quad (5)$$

where T_t denotes a brief reasoning process that explains why certain rows or columns are needed, R and C are the lists of target column headers and row labels, respectively. This formulation encourages the model to reason at the level of table structure, rather than directly accessing cell-level content, enforcing a deliberate *where-to-look* decision before any content is extracted.

Self-refined Sub-table Extraction. The second step performs structure-guided sub-table extraction with self-reflective verification. Instead of directly extracting content from the predicted structural indices, the LVLM is first prompted to assess whether the target rows R and columns C obtained in the previous stage are correct and sufficient for answering the question. Specifically, given the table image V , the question q , and an initial reasoning plan $\{T_t, R, C\}$, the LVLM is instructed with I_{SSE} to explicitly evaluate the adequacy of the plan and revise it if necessary at first, and then extract a minimal sub-table T_{sub} with semi-structured description that contains only the information required to solve the task.

$$T_{sub} = \text{LVLM}(I_{SSE}, \{T_t, R, C\}, V, q). \quad (6)$$

By incorporating self-reflective verification, this step prevents error propagation from imperfect global exploration and enforces a plan-before-extract discipline. The resulting sub-table serves as compact, verifiable evidence, forming a reliable bridge between structural reasoning and final answer generation.

Evidence-grounded Reasoning. Finally, evidence-grounded reasoning is performed to produce the final answer based on explicit and textual visual evidence. Given the extracted sub-table T_{sub} , together with the original table image V and the question q , the LVLM is required to reason over the sub-table as verifiable evidence and generate the final prediction,

$$\hat{y} = \text{LVLM}(I_{EGR}, T_{sub}, V, q), \quad (7)$$

where \hat{y} denotes the predicted answer and I_{EGR} is the corresponding instruction. Rather than reasoning directly over the entire table image, this formulation explicitly constrains the reasoning process to the extracted sub-table, which contains only task-relevant rows and columns. The original table image V is retained as auxiliary context to preserve visual grounding, while the sub-table T_{sub} serves as the primary source of factual evidence.

By grounding reasoning on explicitly extracted evidence, our Table-GLS enforces a clear separation between *evidence selection* and *answer derivation*, reducing spurious correlations and discouraging reliance on global pattern matching. Consequently, the resulting reasoning process is more interpretable and robust for multimodal table understanding. The prompts of each stage are available in Appendix C.

4. Experimental Setup

4.1. Datasets

For table understanding, we first randomly sample 10K table images from various datasets within the pre-training corpus released by Zheng et al. (2024). For each image, we construct paired structure-alignment and content-alignment instances following the proposed DiSCO framework. Then we conduct comprehensive evaluations on the table understanding tasks in MMTab (Zheng et al., 2024), which cover a broad range of table layouts and semantic querying settings, including table size detection (TSD), table cell extraction (TCE), table cell location (TCL), Merged Cell Detection (MCD) and Row&Column Extraction (RCE).

For table reasoning, we focus on representative structure-aware reasoning tasks within MMTab, including five table question answering benchmarks, i.e., WTQ (Pasupat & Liang, 2015), HiTab (Cheng et al., 2022), TAT-QA (Zhu et al., 2021), AIT-QA (Katsis et al., 2022), TabMCQ (Jauhar et al., 2016), and three table fact verification benchmarks, i.e., TabFact (Chen et al., 2020), InfoTabs (Gupta et al., 2020), and PubHealthTab (Akhtar et al., 2022). More details are presented in Appendix D.

4.2. Baselines

For table understanding, we compare DiSCO with conventional multimodal alignment strategies that align table images with serialized **textual** representations, including HTML, Markdown, and LaTeX. To ensure a fair comparison, we report results under two settings, (I) *Textual (10K)*: models aligned using the same 10K table images as DiSCO, and (II) *Textual (97K)*: models trained with the full pre-training data provided by (Zheng et al., 2024), consisting of 97K table images with 150K image-text pairs. We also report the results of TableLlama and Table-LLaVA provided

by Zheng et al. (2024), which are fine-tuned on extensive table-based tasks. For table reasoning, we compare Table-GLS against *open-source LVLMs* without additional fine-tuning, including direct answering (DA) before and after DiSCO alignment. We further report the results from *optimized LVLM*, including Table-LLaVA (Zheng et al., 2024), Table-R1 (Kang et al., 2025), and HIPPO (Liu et al., 2025)². In addition, we include GPT-4o-mini as a *closed-source LVLM* baseline for reference.

4.3. Implementation Details

We fine-tune four representative LVLMs for table alignment, including Gemma3-12B (Team et al., 2025), Gemma3n-E4B-it, LLaVA-v1.6-7B (Liu et al., 2024b), and Qwen3-VL-8B-Instruct (Bai et al., 2025a), with LoRA (Hu et al., 2022) to preserve their original performance and mitigate catastrophic forgetting. For table reasoning, we evaluate Gemma3n-E4B and Qwen3-VL-8B-Instruct with the vLLM (Kwon et al., 2023) framework to ensure efficient inference. All experiments are conducted in a zero-shot setting adhere to Zheng et al. (2024). More details about training and evaluation are shown in Appendix E.

5. Results and Analysis

5.1. Main Results

Table Understanding. Table 1 summarizes the results on multimodal table understanding tasks. Our analysis reveals several key findings: (I) DiSCO consistently enhances table understanding across all evaluated LVLMs and tasks, demonstrating its generalizability beyond specific model architectures or training objectives. (II) The improvements are particularly evident on structure-sensitive tasks such as TSD, TCL, RCE and TCE, suggesting that DiSCO enhances the LVLMs' ability to capture fine-grained row–column semantics. (III) Meanwhile, DiSCO exhibits stronger robustness under OOD settings, especially for size detection and cell extraction tasks, highlighting its ability to generalize to unseen table layouts and distributions. (IV) Compared with *Textual-All*, which leverages the full 150K alignment samples from MMTab, DiSCO achieves comparable or superior performance across most tasks with only 10K table images. This suggests that alignment quality, driven by explicit separation of structure and semantics, is more crucial than data quantity for multimodal table understanding. (V) DiSCO yields consistent improvements across models of different scales. Notably, the larger models, e.g., Qwen3-VL-32B, benefit more substantially, likely

²The results of optimized LVLM are sourced from their original papers. For HIPPO on AIT-QA, TabMCQ, and PubHealthTab, we additionally conduct evaluations using the official released model and scripts.

Table 1. Results on multimodal table understanding tasks. # TI_A indicates the number of table images used for alignment. *None* denotes the original model, *Textual (10K)* and *Textual (97K)* denote the multimodal alignment with textual representations, where the former includes the same 10K table image as in our DISCO and the latter encompasses all alignment data provided by MMTab. *w/o T_L* indicates the removal of the local content alignment. More results are presented in Table 11.

Models	Alignment (# TI_A)	TSD		RCE		MCD	TCE	OOD TSD		OOD TCE	OOD TCL	OOD RCE		
		Row	Column	Row	Column			Row	Column			Row	Column	
TableLlama+Oracle	None	5.30	4.40	0.82	4.34	5.26	-	9.35	-	-	-	-	-	
TableLlama+OCR	None	3.90	3.70	0.65	2.82	2.39	-	3.95	-	-	-	-	-	
Table-LLaVA 7B	Textual (97K)	33.10	33.20	29.31	31.43	37.93	17.14	19.45	25.20	16.40	11.28	26.10	21.97	18.14
Table-LLaVA 13B	Textual (97K)	34.40	27.60	29.68	31.07	41.49	16.52	19.53	31.60	14.80	11.38	26.17	21.94	18.67
Gemma3n-E4B	None	5.50	15.00	8.50	24.82	32.44	1.11	9.02	6.80	18.40	9.00	10.99	19.38	29.77
	Textual (10K)	9.50	19.70	8.30	24.54	23.25	0.71	8.64	10.80	23.60	10.20	12.32	24.20	37.06
	DiSCO w/o T_L (10K)	9.90	20.20	4.71	27.45	23.69	0.76	11.00	12.80	27.20	12.69	7.52	35.86	21.61
	DiSCO (10K)	11.40	20.20	4.66	28.00	31.58	1.79	13.65	14.80	21.60	14.32	6.86	40.56	36.43
Qwen3-VL-8B	None	40.80	75.20	42.00	44.33	72.75	32.79	40.25	43.20	76.80	50.00	42.74	66.61	93.28
	Textual (10K)	41.00	79.60	40.40	52.12	76.74	47.84	40.38	31.20	78.80	50.22	44.81	67.57	82.03
	Textual-All (97K)	37.70	75.80	41.42	50.20	71.66	23.03	45.50	50.40	71.60	59.54	50.07	62.29	86.05
	DiSCO w/o T_L (10K)	44.30	77.60	43.22	55.32	76.23	44.39	43.39	44.40	76.80	51.84	48.67	70.59	88.62
	DiSCO (10K)	42.90	75.90	55.95	56.11	80.50	33.91	56.77	44.40	78.40	65.51	59.12	71.48	84.44
Qwen3-VL-4B	None	28.70	68.90	24.47	29.71	32.00	14.14	12.19	42.00	66.80	14.43	28.70	28.97	0.00
	Textual (10K)	36.60	73.50	37.61	42.22	70.17	13.32	32.04	44.40	69.60	45.66	43.74	33.65	81.46
	DiSCO (10K)	21.70	84.40	52.09	54.88	61.42	22.22	38.30	20.00	76.40	46.85	60.05	51.03	68.46
Qwen3-VL-32B	None	42.00	86.80	55.19	55.84	85.40	57.61	54.09	55.60	83.60	61.61	65.91	69.29	83.53
	Textual (10K)	49.60	89.80	64.38	61.87	89.64	65.78	63.19	54.00	82.80	63.99	70.71	66.11	84.16
	DiSCO (10K)	64.20	93.50	72.04	64.75	89.85	68.40	65.47	66.80	86.80	68.11	74.10	71.70	88.40

Table 2. Ablation study with Qwen3-VL on multimodal table reasoning tasks where *CoT* denotes the vanilla Chain-of-Thought, and *Full* indicates the combination of both DiSCO and Table-GLS. The best result are **bolded**.

Methods	Question Answering		Fact Verification	
	HiTab	AIT-QAO	InfoTabs	PubHealthTab _O
Full	27.35	76.71	72.67	77.14
- GSE	24.30	62.82	72.09	74.92
- SSE	31.41	73.39	70.20	73.94
only Table-GLS	29.76	55.58	73.59	72.76
CoT	28.17	56.75	67.98	57.52
DiSCO+CoT	26.40	73.78	71.00	68.33

because higher-capacity LVLMs can better internalize and exploit disentangled structure and semantic signals when the alignment objectives are explicitly separated.

Table Reasoning. Table 3 reports results on multimodal table reasoning tasks, covering question answering and fact verification under in-domain and out-of-domain settings. The main observations are: (I) Table-GLS outperforms direct answering on almost all benchmarks, highlighting the value of explicit reasoning strategies for table-centric reasoning. (II) After integrating DiSCO, LVLMs show substantial gains in reasoning performance under direct answering settings, particularly for Qwen3-VL with relatively strong inherent table reasoning capabilities. This indicates that DiSCO effectively enhances the inherent implicit structural modeling in LVLMs, enabling better learning of table structure and content for reasoning. (III) Combining DiSCO with Table-GLS achieves the best average score for both Gemma3n and Qwen3-VL, with notable gains on OOD benchmarks such as AIT-

QA and PubHealthTab for Qwen3-VL, indicating the disentangled structure-content alignment provides more reliable evidence grounding, enabling the model to reason more accurately and robustly over unseen tables. (IV) Compared with heavily optimized LVLM, our inference framework achieves comparable performance with minimal supervision. Notably, when combining DiSCO with Table-GLS, the model consistently matches or even surpasses optimized LVLM on several benchmarks, particularly on OOD benchmarks. This indicates that our framework effectively elicits the inherent table reasoning capability of LVLMs without relying on costly task-level fine-tuning.

5.2. Ablation Study

We then examine the contribution of each alignment component in DiSCO. As shown in Table 1, compared with the Textual baseline, DiSCO without local content alignment (i.e., *w/o T_L*) already achieves consistent improvements, indicating that disentangled structure alignment alone substantially enhances table layout understanding. Introducing local content alignment further boosts performance, particularly on structure-sensitive tasks such as TSD, TCL, and RCE, and improves robustness under out-of-domain settings. These results demonstrate that structure alignment and local content grounding are complementary and jointly essential for effective multimodal table understanding.

For Table-GLS, we first conduct ablations on reasoning task by removing the Global Structure Exploration (-GSE) or the Self-refined Sub-table Extraction (-SSE), with results reported in Table 2. Performance consistently drops when either stage is removed, demonstrating the importance of

Table 3. Results on multimodal table reasoning tasks, where $\# TI_R$ indicates the number of table images used for training in the reasoning task and O denotes the out-of-domain dataset that is unseen for all tested methods. The best result among the same category of methods are **bolded**.

Models	Method	# TI_R	Question Answering					Fact Verification			Avg.
			WTQ	HiTab	TAT-QA	AIT-QA $_O$	TabMCQ $_O$	TabFact	InfoTabs	PubHealthTab $_O$	
<i>Closed-Source LVLM</i>											
GPT-4o-mini	DA	0	30.06	20.94	28.37	54.01	36.35	46.54	59.28	48.61	40.52
<i>Optimized LVLM</i>											
Table-LLaVA 7B	SFT	82K	18.43	10.09	12.82	5.48	44.51	59.85	65.26	51.03	33.43
Table-LLaVA 13B	SFT	82K	20.41	10.85	15.67	6.06	51.51	65.00	66.91	48.46	35.61
Qwen2-VL-7B-Table-R1	GRPO	20.6K	50.30	58.20	48.06	-	-	73.40	62.80	-	-
MiniCPM-V-2.6 8B	HIPPO	55.2K	55.77	63.00	60.75	66.14	40.04	82.27	75.74	73.32	64.63
<i>Open-Source LVLM</i>											
Gemma3n-E4B	DA	0	30.50	14.15	22.41	52.25	34.50	41.33	55.04	56.08	38.28
Qwen3-VL-8B	DA	0	49.47	35.47	36.01	71.04	37.71	70.21	45.59	44.18	48.71
<i>Ours</i>											
Gemma3n-E4B-DiSCO	DA	0	24.56	16.81	25.26	64.77	33.24	42.83	52.74	52.47	39.09
	Table-GLS	0	41.32	22.08	33.16	59.10	32.17	55.81	58.76	62.41	45.60
Qwen3-VL-8B-DiSCO	DA	0	50.16	33.50	37.95	75.73	37.80	69.28	63.44	63.34	53.90
	Table-GLS	0	57.11	27.35	40.54	76.71	38.00	75.41	72.67	77.14	58.12

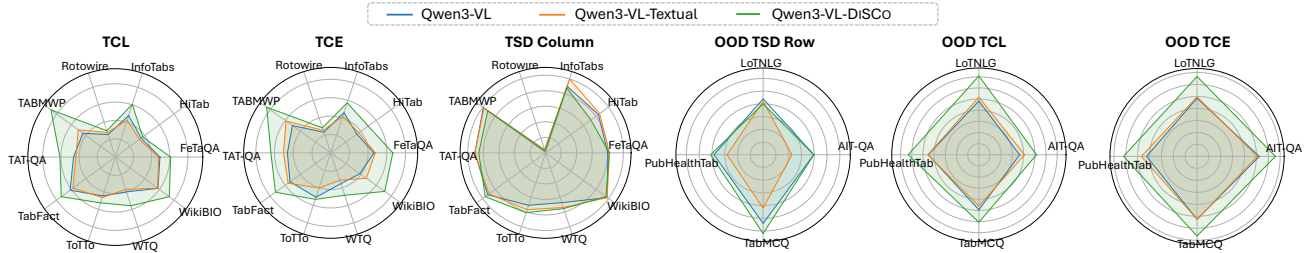


Figure 3. Model performance on representative understanding tasks across various table layouts.

both global structure exploration and sub-table extraction for reliable table reasoning. Notably, eliminating *GSE* leads to substantial drops on all benchmarks, highlighting the necessity of explicitly identifying task-relevant structural regions before reasoning. Interestingly, removing *SSE* slightly improves performance on *HiTab*, likely due to complex nested structures within the table of *HiTab*, where inaccurate sub-table extraction may introduce noisy evidence and hinder reasoning. We also conducted further experiments by directly applying *Table-GLS* to *Qwen3-VL* to evaluate the gains brought by *DiSCO* (*only Table-GLS*). It can be observed a significant performance decline on OOD benchmarks, fully demonstrating that our disentangled alignment enhances LVLMs' capabilities to understand table images, enabling more robust and accurate reasoning on unseen tables. Finally, we further report the results of vanilla Chain-of-Thought with *Qwen3-VL* and *Qwen3-VL-DiSCO*. We can find that our *DiSCO* can also enhance the LVLM's ability to perform step-step reasoning by itself on table reasoning tasks. Meanwhile, compared with *CoT*, *Table-GLS* yields more stable and superior performance across most benchmarks, demonstrating the benefit of structure-guided global-to-local reasoning. We further

analyze the token efficiency of various reasoning strategies in the Appendix G.

5.3. Impact of Table Layouts

To further evaluate the robustness of *DiSCO*, we analyze the performance of *Qwen3-VL-DiSCO* across table layouts of varying scale and structural complexity. As illustrated in Figure 3, *DiSCO* consistently improves the performance of LVLM on most tasks across various table types, with the most significant gains observed in relatively small and compact tables, i.e., *TABMWP* and *WikiBiO*. In high-density tables such as *ToTTo* (average 35 rows) and *Rotowire* (average 33 rows and 19 columns), *DiSCO* demonstrates superior robustness, effectively enhancing model performance across most tasks compared to text representation-based alignment methods. Crucially, the substantial margin maintained on OOD benchmarks, such as *LoTNLG* and *PubHealthTab*, further confirms that our method internalizes the universal logic of tabular organization rather than over-fitting to specific training distributions, thereby efficiently enhancing the LVLM's generalization to unseen layouts. More information about table layouts and results are presented in the Appendix F.

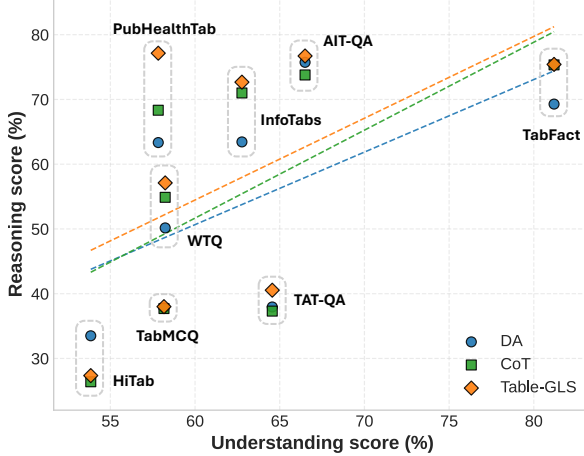


Figure 4. Correlation between table understanding and reasoning performance of Qwen3-VL-DiSCO.

Table 4. Results on non-tabular tasks. The best result are **bolded**.

Models	ScienceQA	CRPE	HallusionBench	TextVQA
MiniCPM-v2.6	95.19	76.32	63.83	75.54
+HIPPO	96.33	76.37	63.41	75.89
Qwen3-VL	94.79	77.68	73.5	80.34
+Textual (10K)	94.94	77.85	72.24	79.91
+DiSCO (10K)	95.09	77.92	74.97	80.83

5.4. Understanding–Reasoning Correlation Analysis

Figure 4 depicts the relationship between table understanding accuracy and downstream reasoning performance on Qwen3-VL after applying DiSCO alignment under different inference strategies. Overall, we observe a clear positive correlation that benchmarks with higher understanding scores consistently yield stronger reasoning performance, indicating that robust table understanding forms a critical foundation for reliable reasoning. Moreover, different reasoning paradigms exhibit distinct sensitivities to understanding quality. Direct Answering exhibits the weakest correlation, as it often bypasses explicit use of table structure and resorts to superficial matching, whereas CoT strengthens the consistency by introducing intermediate reasoning steps that better exploit the LVLM’s structure understanding. Notably, Table-GLS consistently achieves higher reasoning scores at comparable understanding levels, demonstrating that explicitly leveraging structure signals enables the LVLM to more effectively translate understanding gains into reasoning improvements.

5.5. Evaluation on General Reasoning Tasks

To examine the impact of table alignment strategies on general multimodal capabilities, we further evaluate DiSCO on several non-tabular benchmarks: ScienceQA (Lu et al., 2022), hallucination-oriented datasets (CRPE (Wang

et al., 2024) and HallusionBench (Guan et al., 2024)), and the OCR-based TextVQA (Singh et al., 2019). As shown in Table 4, alignment with textual representation (+Textual) exhibits performance degradation on some tasks compared to the original model, indicating that directly aligning table images with full textual representations may introduce alignment bias and over-specialization to linearized table formats, which can negatively affect general visual–language understanding. In contrast, applying DiSCO (+DiSCO) consistently improves performance across all evaluated tasks. And compared to HIPPO, which is optimized based on extensive reasoning data, our DiSCO achieves greater improvements in base model. This suggests that disentangling structure abstraction from semantic grounding helps the LVLM form explicit and reusable internal representations of structure and content, thereby eliciting its intrinsic reasoning capability rather than relying on superficial pattern matching. Consequently, the learned inductive biases transfer effectively beyond table-specific contexts, leading to more robust and generalizable multimodal reasoning.

6. Case Study

To further demonstrate the effectiveness of our framework, we present a case from WTQ in Figure 5. When using vanilla CoT, Qwen3-VL correctly identifies the relevant row but fails to ground the reasoning in accurate content evidence, leading to an incorrect arithmetic operation and a wrong final answer. This highlights the LVLM’s limited ability to reliably exploit table content without structure-aware guidance. In contrast, applying Table-GLS directly enforces a structured reasoning process, enabling the model to successfully localize the relevant row and result cell. However, without enhanced table representations, the extracted evidence is still imperfectly grounded, resulting in an erroneous reasoning. Finally, combining DiSCO with Table-GLS yields correct and interpretable reasoning. DiSCO enables the LVLM to more accurately understand table structure and content through disentangled alignment, allowing Table-GLS to precisely identify task-relevant rows and columns, extract clean sub-table evidence, and perform evidence-grounded reasoning. This example validate how disentangled structure–content alignment and global-to-local reasoning jointly enhance robustness and interpretability in multimodal table reasoning.

7. Conclusion

In this work, we introduce an efficient framework for multimodal table understanding and reasoning that enhances LVLMs without relying on large-scale annotations or external tools. Through disentangled structure–content alignment and lightweight structure-guided global-to-local

reasoning, our framework effectively transfers LVLMs' intrinsic reasoning ability to tables. Extensive experiments demonstrate strong performance and robustness across diverse table tasks, highlighting a scalable and data-efficient solution for multimodal table reasoning.

Impact Statements

This paper presents work whose goal is to advance the research on multimodal table reasoning with large vision-language models. There are many potential societal consequences of our work, none of which we feel must be specifically highlighted here.

References

Akhtar, M., Cocarascu, O., and Simperl, E. PubHealthTab: A public health table-based dataset for evidence-based fact checking. In *Findings of the Association for Computational Linguistics: NAACL 2022*, pp. 1–16, 2022.

Alayrac, J.-B., Donahue, J., Luc, P., Miech, A., Barr, I., Hasson, Y., Lenc, K., Mensch, A., Millican, K., Reynolds, M., et al. Flamingo: a visual language model for few-shot learning. *Advances in neural information processing systems*, 35:23716–23736, 2022.

Bai, S., Cai, Y., Chen, R., Chen, K., Chen, X.-H., Cheng, Z., Deng, L., Ding, W., Fang, R., Gao, C., Ge, C., Ge, W., Guo, Z., Huang, Q., Huang, J., Huang, F., Hui, B., Jiang, S., Li, Z., Li, M., Li, M., Li, K., Lin, Z., Lin, J., Liu, X., Liu, J., Liu, C., Liu, Y., Liu, D., Liu, S., Lu, D., Luo, R., Lv, C., Men, R., Meng, L., Y., Ren, X., yi Ren, X., Song, S., Sun, Y.-C., Tang, J., Tu, J., Wan, J., Wang, P., Wang, P., Wang, Q., Wang, Y., Xie, T., Xu, Y., Xu, H., Xu, J., Yang, Z., Yang, M., Yang, J., Yang, A., Yu, B., Zhang, F., Zhang, H., Zhang, X., Zheng, B., Zhong, H., Zhou, J., Zhou, F., Zhou, J., Zhu, Y., and Zhu, K. Qwen3-vl technical report. *arXiv preprint arXiv:2511.21631*, 2025a.

Bai, S., Chen, K., Liu, X., Wang, J., Ge, W., Song, S., Dang, K., Wang, P., Wang, S., Tang, J., et al. Qwen2.5-vl technical report. *arXiv preprint arXiv:2502.13923*, 2025b.

Borisov, V., Leemann, T., Seßler, K., Haug, J., Pawelczyk, M., and Kasneci, G. Deep neural networks and tabular data: A survey. *IEEE transactions on neural networks and learning systems*, 35(6):7499–7519, 2022.

Chen, W., Wang, H., Chen, J., Zhang, Y., Wang, H., Li, S., Zhou, X., and Wang, W. Y. Tabfact: A large-scale dataset for table-based fact verification. In *International Conference on Learning Representations*, 2020.

Chen, Z., Chen, W., Smiley, C., Shah, S., Borova, I., Langdon, D., Moussa, R., Beane, M., Huang, T.-H., Routledge, B., and Wang, W. Y. FinQA: A dataset of numerical reasoning over financial data. In *Proceedings of the 2021 Conference on Empirical Methods in Natural Language Processing*, pp. 3697–3711, 2021.

Cheng, K., YanTao, L., Xu, F., Zhang, J., Zhou, H., and Liu, Y. Vision-language models can self-improve reasoning via reflection. In *Proceedings of the 2025 Conference of the Nations of the Americas Chapter of the Association for Computational Linguistics: Human Language Technologies (Volume 1: Long Papers)*, pp. 8876–8892, 2025.

Cheng, Z., Dong, H., Wang, Z., Jia, R., Guo, J., Gao, Y., Han, S., Lou, J.-G., and Zhang, D. HiTab: A hierarchical table dataset for question answering and natural language generation. In *Proceedings of the 60th Annual Meeting of the Association for Computational Linguistics (Volume 1: Long Papers)*, pp. 1094–1110, 2022.

Fu, X., Liu, M., Yang, Z., Corring, J. R., Lu, Y., Yang, J., Roth, D., Florencio, D., and Zhang, C. Refocus: Visual editing as a chain of thought for structured image understanding. In *Forty-second International Conference on Machine Learning*, 2025.

Guan, T., Liu, F., Wu, X., Xian, R., Li, Z., Liu, X., Wang, X., Chen, L., Huang, F., Yacoob, Y., et al. Hallusionbench: an advanced diagnostic suite for entangled language hallucination and visual illusion in large vision-language models. In *Proceedings of the IEEE/CVF Conference on Computer Vision and Pattern Recognition*, pp. 14375–14385, 2024.

Gupta, V., Mehta, M., Nokhiz, P., and Srikumar, V. INFOTABS: Inference on tables as semi-structured data. In *Proceedings of the 58th Annual Meeting of the Association for Computational Linguistics*, pp. 2309–2324, 2020.

Herzig, J., Nowak, P. K., Müller, T., Piccinno, F., and Eisenschlos, J. TaPas: Weakly supervised table parsing via pre-training. In *Proceedings of the 58th Annual Meeting of the Association for Computational Linguistics*, pp. 4320–4333, 2020.

Hu, E. J., yelong shen, Wallis, P., Allen-Zhu, Z., Li, Y., Wang, S., Wang, L., and Chen, W. LoRA: Low-rank adaptation of large language models. In *International Conference on Learning Representations*, 2022.

Iida, H., Thai, D., Manjunatha, V., and Iyyer, M. TABBIE: Pretrained representations of tabular data. In *Proceedings of the 2021 Conference of the North American Chapter of the Association for Computational Linguistics: Human Language Technologies*, pp. 3446–3456, 2021.

Jauhar, S. K., Turney, P., and Hovy, E. Tabmcq: A dataset of general knowledge tables and multiple-choice questions. *arXiv preprint arXiv:1602.03960*, 2016.

Jiang, J.-P., Xia, Y., Sun, H.-L., Lu, S., Chen, Q.-G., Luo, W., Zhang, K., Zhan, D.-C., and Ye, H.-J. Multimodal tabular reasoning with privileged structured information. *arXiv preprint arXiv:2506.04088*, 2025.

Kang, X., Wu, S., Wang, Z., Liu, Y., Jin, X., Huang, K., Wang, W., Yue, Y., Huang, X., and Wang, Q. Can GRPO boost complex multimodal table understanding? In *Proceedings of the 2025 Conference on Empirical Methods in Natural Language Processing*, pp. 12642–12655, 2025.

Katsis, Y., Chemmengath, S., Kumar, V., Bharadwaj, S., Canim, M., Glass, M., Gliozzo, A., Pan, F., Sen, J., Sankaranarayanan, K., et al. Ait-qa: Question answering dataset over complex tables in the airline industry. In *Proceedings of the 2022 Conference of the North American Chapter of the Association for Computational Linguistics: Human Language Technologies: Industry Track*, pp. 305–314, 2022.

Kwon, W., Li, Z., Zhuang, S., Sheng, Y., Zheng, L., Yu, C. H., Gonzalez, J., Zhang, H., and Stoica, I. Efficient memory management for large language model serving with pagedattention. In *Proceedings of the 29th Symposium on Operating Systems Principles*, pp. 611–626, 2023.

Li, L., Wang, Y., Xu, R., Wang, P., Feng, X., Kong, L., and Liu, Q. Multimodal ArXiv: A dataset for improving scientific comprehension of large vision-language models. In *Proceedings of the 62nd Annual Meeting of the Association for Computational Linguistics (Volume 1: Long Papers)*, pp. 14369–14387, 2024.

Liu, H., Li, C., Li, Y., and Lee, Y. J. Improved baselines with visual instruction tuning. In *Proceedings of the IEEE/CVF conference on computer vision and pattern recognition*, pp. 26296–26306, 2024a.

Liu, H., Li, C., Li, Y., Li, B., Zhang, Y., Shen, S., and Lee, Y. J. Llava-next: Improved reasoning, ocr, and world knowledge, January 2024b. URL <https://llava-vl.github.io/blog/2024-01-30-llava-next/>.

Liu, Q., Chen, B., Guo, J., Ziyadi, M., Lin, Z., Chen, W., and Lou, J.-G. TAPEX: Table pre-training via learning a neural SQL executor. In *International Conference on Learning Representations*, 2022.

Liu, Z., Wang, H., Li, X., Xiong, Q., Yang, X., Gu, Y., Yan, Y., Shi, Q., Li, F., Yu, G., et al. Hippo: Enhancing the table understanding capability of large language models through hybrid-modal preference optimization. *arXiv preprint arXiv:2502.17315*, 2025.

Lu, P., Mishra, S., Xia, T., Qiu, L., Chang, K.-W., Zhu, S.-C., Tafjord, O., Clark, P., and Kalyan, A. Learn to explain: Multimodal reasoning via thought chains for science question answering. In *Advances in Neural Information Processing Systems*, volume 35, pp. 2507–2521, 2022.

Lu, W., Zhang, J., Fan, J., Fu, Z., Chen, Y., and Du, X. Large language model for table processing: A survey. *Frontiers of Computer Science*, 19(2):192350, 2025.

Pasupat, P. and Liang, P. Compositional semantic parsing on semi-structured tables. In *Proceedings of the 53rd Annual Meeting of the Association for Computational Linguistics and the 7th International Joint Conference on Natural Language Processing (Volume 1: Long Papers)*, pp. 1470–1480, 2015.

Singh, A., Natarajan, V., Shah, M., Jiang, Y., Chen, X., Batra, D., Parikh, D., and Rohrbach, M. Towards vqa models that can read. In *Proceedings of the IEEE/CVF Conference on Computer Vision and Pattern Recognition (CVPR)*, June 2019.

Sui, Y., Zhou, M., Zhou, M., Han, S., and Zhang, D. Table meets llm: Can large language models understand structured table data? a benchmark and empirical study. In *Proceedings of the 17th ACM International Conference on Web Search and Data Mining*, pp. 645–654, 2024.

Team, G., Kamath, A., Ferret, J., Pathak, S., Vieillard, N., Merhej, R., Perrin, S., Matejovicova, T., Ramé, A., Rivière, M., et al. Gemma 3 technical report. *arXiv preprint arXiv:2503.19786*, 2025.

Titiya, P. Y., Trivedi, J., Baral, C., and Gupta, V. Mmtbench: A unified benchmark for complex multimodal table reasoning. *arXiv preprint arXiv:2505.21771*, 2025.

Wang, W., Ren, Y., Luo, H., Li, T., Yan, C., Chen, Z., Wang, W., Li, Q., Lu, L., Zhu, X., et al. The all-seeing project v2: Towards general relation comprehension of the open world. In *European Conference on Computer Vision*, pp. 471–490. Springer, 2024.

Wang, Z., Dong, H., Jia, R., Li, J., Fu, Z., Han, S., and Zhang, D. Tuta: Tree-based transformers for generally structured table pre-training. In *Proceedings of the 27th ACM SIGKDD Conference on Knowledge Discovery & Data Mining*, pp. 1780–1790, 2021.

Zhao, W., Feng, H., Liu, Q., Tang, J., Wu, B., Liao, L., Wei, S., Ye, Y., Liu, H., Zhou, W., et al. Tabpedia: Towards comprehensive visual table understanding with concept synergy. *Advances in Neural Information Processing Systems*, 37:7185–7212, 2024.

Zheng, M., Feng, X., Si, Q., She, Q., Lin, Z., Jiang, W., and Wang, W. Multimodal table understanding. In *Proceedings of the 62nd Annual Meeting of the Association for Computational Linguistics (Volume 1: Long Papers)*, pp. 9102–9124, 2024.

Zhou, B., Gao, Z., Wang, Z., Zhang, B., Wang, Y., Chen, Z., and Xie, H. Syntab-llava: Enhancing multimodal table understanding with decoupled synthesis. In *Proceedings of the IEEE/CVF Conference on Computer Vision and Pattern Recognition (CVPR)*, pp. 24796–24806, June 2025.

Zhu, F., Lei, W., Huang, Y., Wang, C., Zhang, S., Lv, J., Feng, F., and Chua, T.-S. TAT-QA: A question answering benchmark on a hybrid of tabular and textual content in finance. In *Proceedings of the 59th Annual Meeting of the Association for Computational Linguistics and the 11th International Joint Conference on Natural Language Processing (Volume 1: Long Papers)*, pp. 3277–3287, 2021.

Zhu, Y., Bai, X., Chen, K., Xiang, Y., Yu, J., and Zhang, M. Benchmarking and improving large vision-language models for fundamental visual graph understanding and reasoning. In *Proceedings of the 63rd Annual Meeting of the Association for Computational Linguistics (Volume 1: Long Papers)*, pp. 30678–30701, 2025.

Limitations

While our framework achieves strong performance with high scalability and data efficiency, it still has several limitations.

- First, DiSCO still relies on the availability of the table structure–content decoupled data, and its effectiveness may vary when table layouts are extremely irregular or implicitly encoded.
- Second, although Table-GLS avoids external tools, its multi-stage reasoning introduces additional token generation compared to direct answering, which may increase inference cost in latency-sensitive settings.
- Finally, our study focuses on table-centric reasoning tasks; extending the proposed framework to more general structured visual reasoning scenarios remains an open direction for future work.

A. Case Study

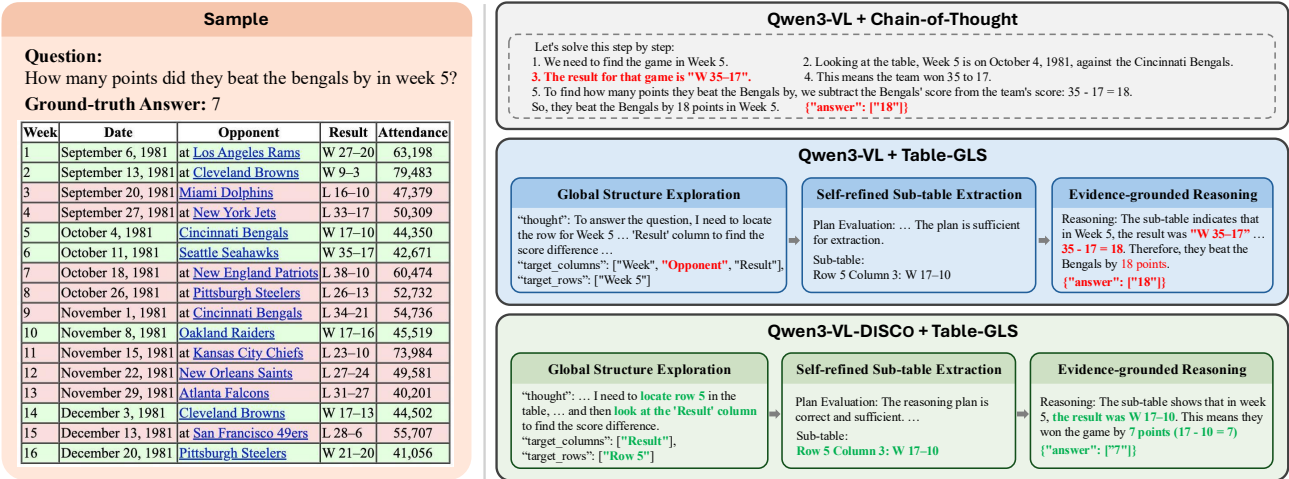


Figure 5. An example of multimodal table reasoning task.

B. Data Construction for DiSCO

We first randomly sample 10K table images from various datasets within the pre-training corpus released by Zheng et al. (2024). For each image, we construct paired structure-alignment and content-alignment instances following the proposed DiSCO framework, yielding a total of 30K image-text pairs for training.

Structure Alignment. We first replace the content information in the HTML, Markdown, or LaTeX representations corresponding to the table images with `[table content]`, retaining only the structural information. Then, we append **“Replace all the table contents with ‘[table content]’, keeping the table structure intact.”** to the original queries provided by Zheng et al. (2024). The final data for structure alignment is constructed by combining the new query with its corresponding anonymized structure representation.

Global Content Alignment. We generated natural language descriptions for each table image, including the total number of rows and columns as well as the content of each cell, formatted as follows:

The table has m rows and n columns
Row 1 Column 1: cell content
Row 1 Column 2: cell content
.....
Row m Column n: cell content

To increase the diversity of samples, we design various instructions with similar semantics for global content alignment.

- <image>\nDescribe the table shown in the image in the following format.\nThe table has [m] rows and [n] columns.\nRow 1 Column 1: [Content]\nRow 1 Column 2: [Content]\n...\nRow m Column n: [Content]\n
- <image>\nDescribe the structure and content of the table in the image, listing each cell's information in the specified format.\nThe table has [m] rows and [n] columns.\nRow 1 Column 1: [Content]\nRow 1 Column 2: [Content]\n...\nRow m Column n: [Content]\n
- <image>\nProvide a thorough description of the table depicted in the image, including its dimensions and the content of each cell, following the format below.\nThe table has [m] rows and [n] columns.\nRow 1 Column 1: [Content]\nRow 1 Column 2: [Content]\n...\nRow m Column n: [Content]\n
- <image>\nExamine the table in the image and produce a comprehensive description that includes the number of rows and columns, as well as the content of each cell, formatted as shown.\nThe table has [m] rows and [n] columns.\nRow 1 Column 1: [Content]\nRow 1 Column 2: [Content]\n...\nRow m Column n: [Content]\n
- <image>\nTransform the table shown in the image into a detailed textual format, specifying the number of rows and columns, along with the content of each cell as illustrated below.\nThe table has [m] rows and [n] columns.\nRow 1 Column 1: [Content]\nRow 1 Column 2: [Content]\n...\nRow m Column n: [Content]\n
- <image>\nConvert the table displayed in the image into a detailed text description, adhering to the format provided below.\nThe table has [m] rows and [n] columns.\nRow 1 Column 1: [Content]\nRow 1 Column 2: [Content]\n...\nRow m Column n: [Content]\n
- <image>\nGenerate a structured textual representation of the table in the image, detailing each cell's content in the specified format.\nThe table has [m] rows and [n] columns.\nRow 1 Column 1: [Content]\nRow 1 Column 2: [Content]\n...\nRow m Column n: [Content]\n
- <image>\nAnalyze the table in the image and output a detailed textual description listing every cell in the following format.\nThe table has [m] rows and [n] columns.\nRow 1 Column 1: [Content]\nRow 1 Column 2: [Content]\n...\nRow m Column n: [Content]\n
- <image>\nRead the table content from the image and reconstruct its structure in text form as shown below.\nThe table has [m] rows and [n] columns.\nRow 1 Column 1: [Content]\nRow 1 Column 2: [Content]\n...\nRow m Column n: [Content]\n
- <image>\nProvide a detailed description of the table in the image, including the number of rows and columns, as well as the content of each cell, following the format below.\nThe table has [m] rows and [n] columns.\nRow 1 Column 1: [Content]\nRow 1 Column 2: [Content]\n...\nRow m Column n: [Content]\n

Local Content Alignment. We randomly select the cell at row m , column n in the table and ask the model for its content. The corresponding label is “*Row m Column n : cell content*”. We also generate 10 semantically similar instructions to enhance diversity.

- What is the exact value located at Row $\{R\}$ and Column $\{C\}$?
- Retrieve the content of the cell at coordinate Row $\{R\}$, Column $\{C\}$.
- Perform a lookup for the data point at index Row $\{R\}$, Column $\{C\}$.
- Identify the specific data found in cell Row $\{R\}$, Column $\{C\}$.
- State the information present at Row index $\{R\}$ and Column index $\{C\}$.
- Read the exact data from the cell defined by Row $\{R\}$ and Column $\{C\}$.
- Query the table for the value at the coordinate (Row $\{R\}$, Column $\{C\}$).

- In the grid, what is present at the intersection of Row {R} and Column {C}?
- Return the single data point located at Row {R}, Column {C}.
- Content of the cell with indices Row {R}, Column {C}.

C. Prompts for Table-GLS

Global Structure Exploration I_{GSE}

You are given a table image and a question.
 Your task is to analyze the layout and headers of the table to locate the information needed to answer the given question.

Please output in the following JSON format:

```
{}  

  "thought": "Briefly explain your reasoning on which columns/rows are needed.",  

  "target_columns": ["List the exact column headers required"],  

  "target_rows": ["List the target row labels required"] or "Describe the condition  

  to filter rows (e.g., 'Year is 2023 or 2024')",  

{}  

Question:  

{question}
```

Self-refined Sub-table Extraction I_{SSE}

You are given a table image, a question and a reasoning plan with target rows and columns.

First, evaluate whether the given reasoning plan is correct and sufficient for answering the question. If the plan is incorrect or incomplete, revise it to obtain a correct reasoning plan.

Then, based on the correct reasoning plan, extract the sub-table that is necessary to answer the question.

Output strictly in the following format:
 Plan Evaluation: "brief explanation of your judgment"
 Sub-table:
 Row m Column n: [Content]

...

Reasoning Plan:
{reasoning_plan}

Question:
{question}

Evidence-grounded Reasoning. I_{EGR}

You are given a table image, a question and a sub-table.
 First, let's think step by step based on the given information.
 Then provide the final concise answer in the JSON format `>{"answer": "<YOUR ANSWER>"}`.

Output in the following format:

Reasoning: "think step by step to answer the question"
`>{"answer": "<YOUR ANSWER>"}`

Sub-table:
`{subtable}`

Question:
`{question}`

D. Datasets

The statistics of table type used for DiSCO alignment are shown in Table 5.

Table 5. The statistics of DiSCO alignment data, where *# Tables* and *# Samples* indicated the number of table images and samples, respectively.

Benchmarks	TABMWP	WTQ	FeTaQA	HiTab	TAT-QA	TabFact	InfoTabs	ToTTo	Rotowire	WikiBIO
# Tables	2623	101	539	397	360	1694	123	2780	671	346
# Samples	8088	303	1617	1191	1134	5415	369	8691	2154	1038

The statistics of evaluation data for multimodal table understanding are shown in Table 6.

Table 6. The statistics of multimodal table understanding data, where *# Tables* and *# Samples* indicated the number of table images and samples, respectively.

Task	TSD	TCL	RCE	MCD	TCE	OOD_TSD	OOD_TCL	OOD_RCE	OOD_TCE
# Tables	1000	1000	1000	1000	1000	250	250	250	250
# Samples	1000	1000	1000	1000	1000	250	250	250	250

The statistics of evaluation data for multimodal table reasoning are shown in Table 7.

Table 7. The statistics of multimodal table reasoning data, where *# Tables* and *# Samples* indicated the number of table images and samples, respectively.

Benchmark	WTQ	HiTab	TAT-QA	TabFact	InfoTabs	TabMCQ	AIT-QA	PubHealthTab
# Tables	421	535	231	1045	600	50	111	362
# Samples	4344	1576	772	6845	5400	1029	511	1942

E. Implementation Details

The hyperparameters for DiSCO alignment training are shown in Table 8.

Table 8. Hyperparameters for DiSCO alignment training.

Models	Lora_rank	Lora_alpha	Global Batch Size	Learning rate	Epoch
Gemma3-12B	8	16	64	1e-4	1
LLaVA-v1.6-7B	8	16	64	1e-4	1
Gemma3n-E4B	8	16	64	1e-5	1
Qwen3-VL-8B	8	16	64	4e-5	1

For multimodal table understanding tasks, we directly use the query provided by MMTab for testing. For table reasoning tasks, we append “*Provide the answer in the JSON format { “answer”: “<YOUR ANSWER>”} directly without any other explanation.*” and “*Think step by step and output the final answer in the JSON format { “answer”: “<YOUR ANSWER>”}*” after the original question from each benchmark (for TQA tasks) or the query provided by MMTab (for TFV tasks) for direct answering and chain-of-thought, respectively.

Following [Zheng et al. \(2024\)](#), we use accuracy for the evaluation of table question answering and fact verification tasks. For TSD, we compute accuracy for the predicted row count and column count separately. For TCE and TCL, we calculate the accuracy at cell level. For MCD, we apply the cell-level F1 score. And for RCE, we compute the cell-level F1 score separately for the extracted rows and columns. All the experiments are finished on 4 NVIDIA H20 GPUs with 96GB memory.

F. Impact of Table Layouts

We first analyze the scale of tables associated with each benchmark in MMTab, and then manually assign a complexity level (high/medium/low) to each table based on its structure, such as scale, header nesting, and cell-merging characteristics. The results are shown in Table 9.

Table 9. The statistics of the scale and complexity of tables in each benchmark.

Benchmarks	LoTNLG	TABMWP	HiTab	TabFact	TAT-QA	Rotowire	InfoTabs	AIT-QA	PubHealthTab	TabMCQ	FeTaQA	ToTTo	HiTab.t2t	WikibIO	WTQ
Avg. Rows	14.49	6.45	19.37	14.07	9.73	32.63	11.21	13.39	9.24	13.62	15.16	34.97	22.38	9.70	27.78
Avg. Cols	6.18	2.19	9.84	6.24	3.92	19.00	2.04	5.50	3.87	4.10	5.70	6.71	8.16	3.02	6.33
Complexity	Medium	Low	High	Medium	Low	High	Low	High	Low	Low	Medium	High	High	Low	High

Figure 6 illustrates additional experimental results on multimodal table understanding performance across various table layouts. Overall, the observed trends are consistent with those in the main paper, showing that DiSCO brings stable improvements across different table layouts, with more pronounced gains on unseen tables.

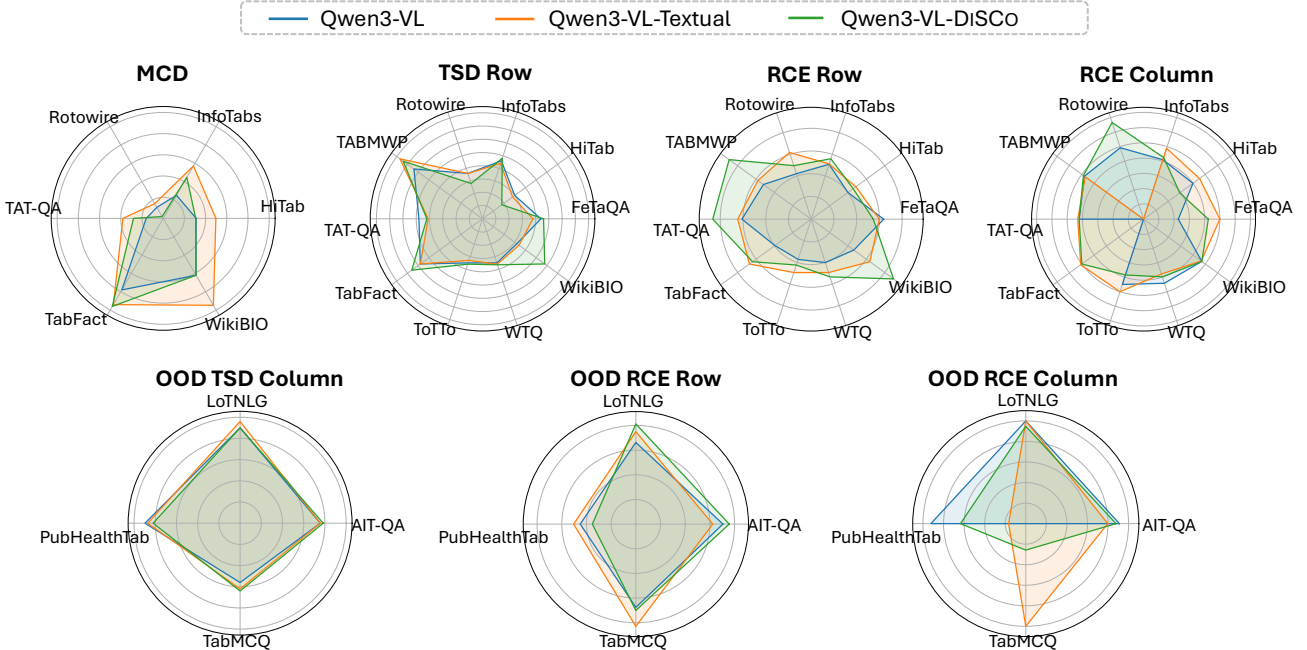


Figure 6. Model performance on representative understanding tasks across various table layouts.

G. Token Efficient Analysis

Table 10 reports the average number of tokens generated during inference under different reasoning strategies. Overall, CoT-based method produces relatively short reasoning traces, while Table-GLS introduces longer outputs due to its explicit multi-stage global-to-local reasoning process. Notably, incorporating DiSCO consistently reduces the token length for vanilla CoT across all benchmarks, indicating that structure–content disentangled alignment enables more concise and focused reasoning. For Table-GLS, DiSCO slightly increases token usage on some benchmarks, reflecting richer and more explicit structural exploration and sub-table verification. Notably, this increase is not uniform and remains controlled across tasks. Therefore, these results suggest that DiSCO improves reasoning efficiency by reducing redundant generation in free-form reasoning, while complementing Table-GLS with more structured and interpretable reasoning traces rather than indiscriminately increasing verbosity.

Table 10. The statistics of the scale and complexity of tables in each benchmark.

Methods	WTQ	HiTab	TAT-QA	TabFact	InfoTabs	TabMCQ	AIT-QA	PubHealthTab	Avg
CoT	337.73	281.50	221.75	317.63	191.75	213.71	219.25	181.92	240.79
DiSCO+CoT	248.59	230.63	194.38	230.79	116.49	141.83	215.53	128.42	189.34
Table-GLS	719.73	424.44	421.70	559.16	356.61	361.52	341.41	385.60	439.45
DiSCO+Table-GLS	727.58	539.53	373.85	696.35	539.63	325.21	355.46	493.41	492.37

Table 11. Complete results on multimodal table understanding tasks. *None* denotes the original model, *Textual* and *Textual-All* denote the multimodal alignment with textual representations, i.e., HTML, Markdown and LaTeX, where the former includes **the same table image** as in our DiSCO and the latter encompasses all alignment data provided by MMTab. *w/o T_L* indicates the removal of the local content alignment.

Models	Alignment	TSD		RCE		MCD	TCE	OOD TSD		OOD TCE	OOD TCL	OOD RCE		
		Row	Column	Row	Column			Row	Column			Row	Column	
TableLlama+Oracle	None	5.30	4.40	0.82	4.34	5.26	-	9.35	-	-	-	-	-	
TableLlama+OCR	None	3.90	3.70	0.65	2.82	2.39	-	3.95	-	-	-	-	-	
Table-LLaVA 7B	Textual-All	33.10	33.20	29.31	31.43	37.93	17.14	19.45	25.20	16.40	11.28	26.10	21.97	18.14
Table-LLaVA 13B	Textual-All	34.40	27.60	29.68	31.07	41.49	16.52	19.53	31.60	14.80	11.38	26.17	21.94	18.67
Gemma3-12B	None	12.40	33.10	3.01	25.46	47.65	2.41	9.26	15.20	40.80	8.46	2.86	21.62	56.95
	Textual	12.00	30.00	4.33	26.32	46.94	0.52	9.34	18.80	34.40	10.41	6.46	32.35	63.89
	DiSCO w/o T_L	21.30	37.90	15.50	28.79	46.22	2.45	17.90	25.20	45.20	22.78	21.70	33.10	64.23
	DiSCO	20.30	33.00	17.25	43.65	54.47	2.84	21.53	28.80	34.80	26.14	20.34	42.31	71.39
LLaVA-v1.6-7B	None	2.50	5.40	1.05	10.91	10.72	0.51	3.52	3.60	6.00	3.47	1.26	14.25	9.27
	Textual	3.40	10.70	4.10	17.07	10.82	0.27	2.65	2.40	8.40	2.82	2.53	22.60	11.34
	DiSCO w/o T_L	5.20	10.80	1.70	16.43	14.95	0.00	5.07	7.60	6.40	6.07	1.80	33.02	13.33
	DiSCO	12.20	20.20	2.84	18.76	8.30	0.02	16.28	13.20	15.60	18.98	2.73	28.00	9.35
Gemma3n-E4B	None	5.50	15.00	8.50	24.82	32.44	1.11	9.02	6.80	18.40	9.00	10.99	19.38	29.77
	Textual	9.50	19.70	8.30	24.54	23.25	0.71	8.64	10.80	23.60	10.20	12.32	24.20	37.06
	DiSCO w/o T_L	9.90	20.20	4.71	27.45	23.69	0.76	11.00	12.80	27.20	12.69	7.52	35.86	21.61
	DiSCO	11.40	20.20	4.66	28.00	31.58	1.79	13.65	14.80	21.60	14.32	6.86	40.56	36.43
Qwen3-VL-8B	None	40.80	75.20	42.00	44.33	72.75	32.79	40.25	43.20	76.80	50.00	42.74	66.61	93.28
	Textual	41.00	79.60	40.40	52.12	76.74	47.84	40.38	31.20	78.80	50.22	44.81	67.57	82.03
	Textual-All	37.70	75.80	41.42	50.20	71.66	23.03	45.50	50.40	71.60	59.54	50.07	62.29	86.05
	DiSCO w/o T_L	44.30	77.60	43.22	55.32	76.23	44.39	43.39	44.40	76.80	51.84	48.67	70.59	88.62
	DiSCO	42.90	75.90	55.95	56.11	80.50	33.91	56.77	44.40	78.40	65.51	59.12	71.48	84.44
Qwen3-VL-4B	None	28.70	68.90	24.47	29.71	32.00	14.14	12.19	42.00	66.80	14.43	28.70	28.97	0.00
	Textual	36.60	73.50	37.61	42.22	70.17	13.32	32.04	44.40	69.60	45.66	43.74	33.65	81.46
	DiSCO	21.70	84.40	52.09	54.88	61.42	22.22	38.30	20.00	76.40	46.85	60.05	51.03	68.46
Qwen3-VL-32B	None	42.00	86.80	55.19	55.84	85.40	57.61	54.09	55.60	83.60	61.61	65.91	69.29	83.53
	Textual	49.60	89.80	64.38	61.87	89.64	65.78	63.19	54.00	82.80	63.99	70.71	66.11	84.16
	DiSCO	64.20	93.50	72.04	64.75	89.85	68.40	65.47	66.80	86.80	68.11	74.10	71.70	88.40